

Increased Pulmonary Pneumococcal Clearance after Resolution of H9N2 Avian Influenza Virus Infection in Mice

Jingyun Li,^a Hongyan Wang,^{a*} Pengjing Lian,^a Yu Bai,^a Zihui Zhang,^a Lihong Zhao,^a Tong Xu,^b Jian Qiao^a

^aDepartment of Pathophysiology, College of Veterinary Medicine, China Agricultural University, Beijing, China

^bDepartment of Veterinary Medicine, College of Animal Science, Hebei North University, Zhangjiakou, Hebei Province, China

ABSTRACT H9N2 avian influenza virus has been continuously circulating among poultry and can infect mammals, indicating that this virus is a potential pandemic strain. During influenza pandemics, secondary bacterial (particularly pneumococcal) pneumonia usually contributes to excessive mortality. In the present study, we observed the dynamic effect of H9N2 virus infection on host defense against secondary pneumococcal infection in mice. BALB/c mice were intranasally inoculated with 1.2×10^5 PFU of H9N2 virus followed by 1×10^6 CFU of *Streptococcus pneumoniae* at 7, 14, or 28 days post-H9N2 infection (dpi). The bacterial load, histopathology, body weight, and survival were assessed after pneumococcal infection. Our results showed that H9N2 virus infection had no significant impact on host resistance to secondary pneumococcal infection at 7 dpi. However, H9N2 virus infection increased pulmonary pneumococcal clearance and reduced pneumococcal pneumonia-induced morbidity after secondary pneumococcal infection at 14 or 28 dpi, as reflected by significantly decreased bacterial loads, markedly alleviated pulmonary histopathological changes, and significantly reduced weight loss in mice infected with H9N2 virus followed by *S. pneumoniae* compared with mice infected only with *S. pneumoniae*. Further, the significantly decreased bacterial loads were observed when mice were previously infected with a high dose (1.2×10^6 PFU) of H9N2 virus. Also, similar to the results obtained in BALB/c mice, improvement in pulmonary pneumococcal clearance was observed in C57BL/6 mice. Overall, our results showed that pulmonary pneumococcal clearance is improved after resolution of H9N2 virus infection in mice.

KEYWORDS H9N2 virus, *Streptococcus pneumoniae*, secondary bacterial infections, pneumococcal clearance, mice

H9N2 avian influenza virus has become widespread among poultry in many areas of Eurasia and Africa over the last 3 decades and was the dominant subtype isolated from chickens in China during 2016 to 2019 (1, 2). H9N2 virus has also been isolated from pigs, minks, and humans, demonstrating that this virus could cross species barriers to infect mammals (3–5). Several serological surveys have showed that 13.7% to 37.2% of people in China might have been infected with H9N2 virus (6, 7). Moreover, H9N2 virus contributes to the genesis of the novel H7N9, H10N8, and H5N6 viruses, which have been found to cause severe diseases and even fatalities in humans (8–12). The wide prevalence, enlarged range of mammalian hosts, and extensive genetic reassortment underscore the pandemic threat of H9N2 virus to human health (13).

Streptococcus pneumoniae, or pneumococcus, is a common inhabitant of the upper respiratory tract in approximately 20% to 90% of healthy children and 5% to 20% of healthy adults (14, 15). Defects in host defense, however, could alter the normal interactions between *S. pneumoniae* and host and enable *S. pneumoniae* to invade the lung, causing pneumonia. Pneumococcal pneumonia is still a major health problem worldwide despite interventions, including vaccines and antibiotics (16). Influenza virus infection is a well-recognized risk factor for pneumococcal pneumonia. Infections with

Citation Li J, Wang H, Lian P, Bai Y, Zhang Z, Zhao L, Xu T, Qiao J. 2021. Increased pulmonary pneumococcal clearance after resolution of H9N2 avian influenza virus infection in mice. *Infect Immun* 89:e00062-21. <https://doi.org/10.1128/IAI.00062-21>.

Editor Andreas J. Bäuml, University of California, Davis

Copyright © 2021 Li et al. This is an open-access article distributed under the terms of the [Creative Commons Attribution 4.0 International license](https://creativecommons.org/licenses/by/4.0/).

Address correspondence to Jian Qiao, qiaojian@cau.edu.cn.

* Present address: Hongyan Wang, Department of Veterinary Medicine, College of Life Sciences and Food Engineering, Hebei University of Engineering, Handan, Hebei Province, China.

Received 26 February 2021

Accepted 1 March 2021

Accepted manuscript posted online 15 March 2021

Published 17 May 2021

influenza virus followed by bacteria, particularly *S. pneumoniae*, are associated with high morbidity and mortality, which is evident from previous influenza pandemics as well as from seasonal influenza epidemics (17–21). For example, the estimates from clinical and autopsy cases have shown that more than 95% and 50% of severe illnesses and deaths that occurred during the 1918 pandemic and 2009 pandemic, respectively, are due to secondary bacterial (especially pneumococcal) infections (17–20).

Mechanisms of increased susceptibility to secondary bacterial infections following influenza virus infection have been widely studied since the 1918 pandemic (22, 23). Data from animal models indicate that influenza virus infections facilitate bacterial transmission (24), colonization, and infection by impairing tracheal mucociliary clearance (25), damaging the airway epithelium to expose bacterial attachment sites (26, 27), and suppressing lung innate immunity (28). Defects in lung innate immune response, including the loss and dysfunction of alveolar macrophages (29, 30) and neutrophils (31, 32) and the dysregulation of cytokine productions (33), could play a key role in promoting secondary bacterial pneumonia.

However, secondary bacterial infections were mostly performed after a limited set of mouse-adapted laboratory influenza virus infections in previous studies. Secondary bacterial infections following other influenza virus infections have been less studied. Given the pandemic threat of H9N2 virus to human beings and the fact that secondary pneumococcal pneumonia accounts for excessive mortality during influenza pandemics, it is necessary to determine whether H9N2 virus infection predisposes hosts to secondary pneumococcal infection. Thus, the present study was designed to observe the effect of H9N2 virus infection on the host resistance to secondary pneumococcal infection at different time points post-H9N2 infection by utilizing mouse models. Understanding the interplay among H9N2 virus, host, and *S. pneumoniae* may provide better strategies for H9N2 pandemic preparedness. Here, our results showed that H9N2 virus infection did not increase the susceptibility of mice to secondary pneumococcal infection at 7 days post-H9N2 infection and improved pulmonary pneumococcal clearance when secondary pneumococcal infection was performed after resolution of H9N2 virus infection.

RESULTS

H9N2 virus infection caused obvious respiratory diseases in BALB/c mice. After a nonlethal dose (1.2×10^5 PFU) of H9N2 virus infection, BALB/c mice exhibited slight inactivity, chills, ruffled fur, and inappetence at 3 days post-H9N2 infection (dpi) and more severe clinical signs from 5 to 7 dpi. In addition, H9N2-infected mice showed gradual weight loss, reached peak weight loss at 6 dpi, and recovered gradually thereafter (Fig. 1A). The body weight was not significantly different between H9N2-infected mice and mock-infected mice at 10 dpi and afterward (Fig. 1A). The virus was detected in the lungs of H9N2-infected mice at 3 and 7 dpi but not at 14 or 28 dpi (Fig. 1B). Additionally, pronounced bronchiolitis and alveolitis, characterized by extensive inflammatory cellular infiltration around bronchioles, alveoli, and blood vessels, were seen in the lungs of H9N2-infected mice at 7 dpi (Fig. 1C). The overall architecture of the lungs of H9N2-infected mice was similar to those of mock-infected mice at 14 and 28 dpi (Fig. 1C). In line with these observations, the percentage of lung areas affected, determined by semiquantitative measurement of histopathological alterations, was significantly increased in H9N2-infected mice compared with mock-infected mice at 7 dpi but was not significantly different between the two groups at 14 and 28 dpi (Fig. 1D). Altogether, these data showed that H9N2 virus infection caused obvious respiratory diseases in BALB/c mice and that mice infected with H9N2 virus had recovered by 14 dpi.

H9N2 virus infection had no significant impact on host resistance to secondary pneumococcal infection at 7 dpi in BALB/c mice. It is well recognized that 7 days after influenza virus infection is a window of susceptibility to secondary bacterial infections in human and mouse models (34, 35). Therefore, we observed the effect of H9N2 virus infection on the host resistance to secondary pneumococcal infection at 7 dpi in BALB/c mice. As the ability of the lung to clear bacterial pathogens is an important part of the host defense against pulmonary bacterial infections, we first measured the pulmonary bacterial loads at 6 h and

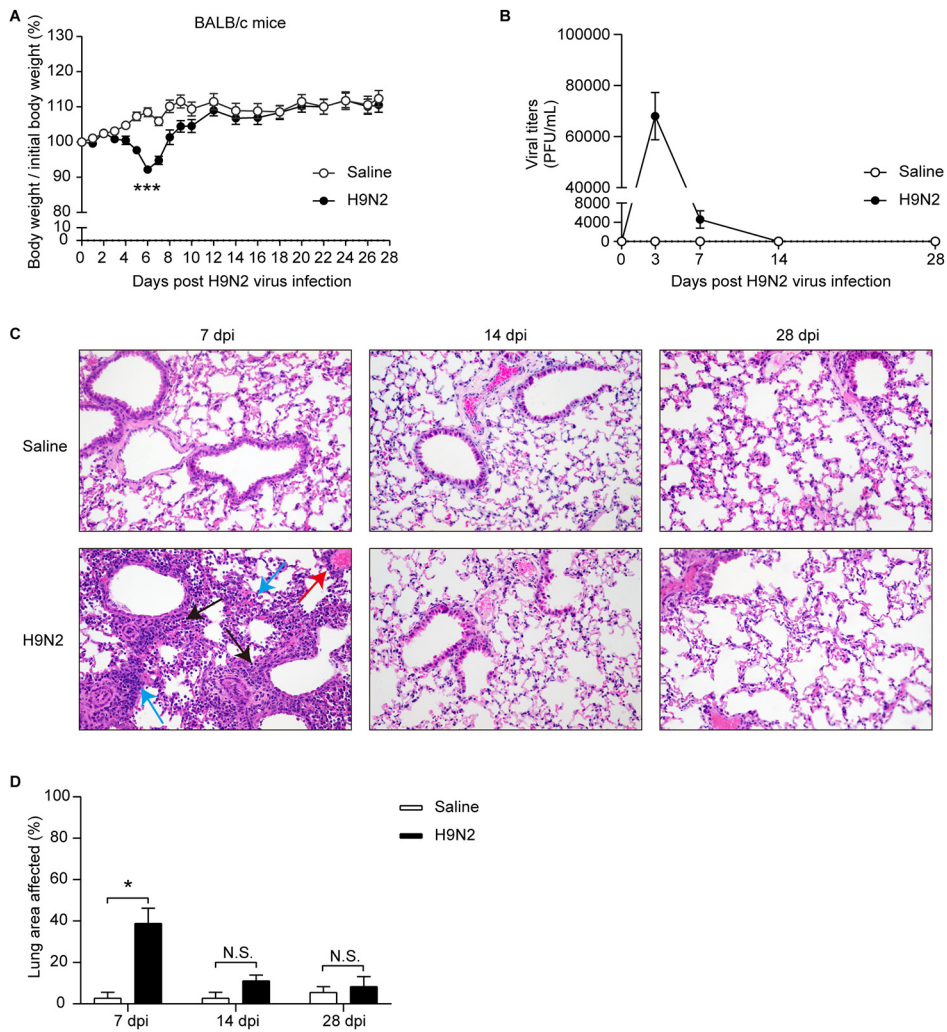


FIG 1 H9N2 virus infection caused obvious respiratory diseases in BALB/c mice. BALB/c mice were intranasally inoculated with 1.2×10^5 PFU of H9N2 virus or with noninfectious allantoic fluid diluted in sterile saline as a control. (A) Body weight changes of mock-infected mice and H9N2-infected mice after H9N2 virus infection ($n = 10$ /group). (B) Viral titers in the lungs of H9N2-infected mice at 3, 7, 14, and 28 dpi ($n = 2$ or 3/group). (C) Representative H&E-stained lung sections (magnification, $\times 400$) of mock-infected mice and H9N2-infected mice at 7, 14, and 28 dpi ($n = 3$ /group). Extensive inflammatory cellular infiltration around bronchioles (black arrows), alveoli (blue arrows), and blood vessels (red arrows) was observed in the lungs of H9N2-infected mice at 7 dpi. (D) Percentage of lung areas affected in mock-infected mice and H9N2-infected mice, calculated from specified histopathological parameters, including peribronchial inflammation, intraalveolar inflammation and perivascular inflammation ($n = 3$ /group). Data are means and SEM. Two-tailed unpaired Student's *t* test was applied for two-group comparisons. *, $P < 0.05$; ***, $P < 0.001$; N.S., not significant.

12 h after infection with 1×10^6 CFU of pneumococci at 7 dpi. No statistically significant differences in pulmonary bacterial loads were found between mice infected with H9N2 virus followed by *S. pneumoniae* (dually infected mice) and mice infected only with *S. pneumoniae* (*S. pneumoniae*-infected mice) (Fig. 2A and B, left).

We then assessed lung histopathology at 6 h after pneumococcal infection at 7 dpi. Pronounced interstitial pneumonia, characterized by denuded epithelia, intra-alveolar fibrin exudation, and extensive inflammatory cell recruitment around bronchioles, alveoli, and blood vessels, was seen in the lungs of mice at 6 h after pneumococcal infection (Fig. 3A). The extents of pulmonary histopathological alterations were similar between dually infected mice and *S. pneumoniae*-infected mice (Fig. 3A and B).

The body weight changes and survival were monitored after a $0.6 \times$ median lethal dose (1×10^8 CFU) of *S. pneumoniae* infection at 7 dpi. The body weight changes after

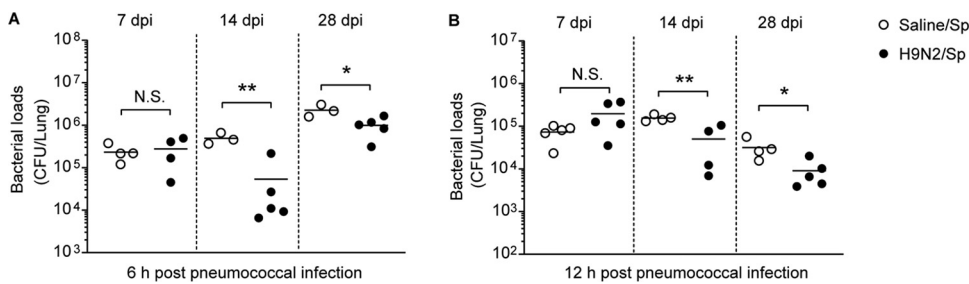


FIG 2 H9N2 virus infection improved pulmonary pneumococcal clearance in BALB/c mice when secondary pneumococcal infection was performed at 14 or 28 dpi. BALB/c mice were intranasally inoculated with 1.2×10^5 PFU of H9N2 virus or with noninfectious allantoic fluid diluted in sterile saline as a control; at 7, 14, or 28 days after H9N2 virus infection, mice were intranasally inoculated with 1×10^6 CFU of *S. pneumoniae*. Bacterial loads in the lungs of *S. pneumoniae*-infected mice and dually infected mice were determined at (A) 6 h and (B) 12 h after pneumococcal infection at 7, 14, or 28 dpi ($n=3$ to 5/group). Data are means and SEM. Two-tailed unpaired Student's *t* test was applied for two-group comparisons. *, $P < 0.05$; **, $P < 0.01$; N.S., not significant; Sp, *Streptococcus pneumoniae*.

pneumococcal infection were showed in Fig. 4A, and the degree of weight loss was not obviously different between dually infected mice and *S. pneumoniae*-infected mice (Table 1). The survival after pneumococcal infection was also not different between dually infected mice and *S. pneumoniae*-infected mice (Fig. 4B). Together, the above results showed that H9N2 virus infection had no significant impact on host resistance to secondary pneumococcal infection at 7 dpi in BALB/c mice.

Preceding H9N2 virus infection increased pulmonary pneumococcal clearance and reduced pneumococcal pneumonia-induced morbidity in BALB/c mice after recovery from influenza. We also observed the effect of H9N2 virus infection on the host resistance to secondary pneumococcal infection at 14 or 28 dpi, when mice infected with H9N2 virus had recovered from influenza. Bacterial loads at 6 h and 12 h after pneumococcal infection at 14 dpi were both significantly decreased in the lungs of dually infected mice compared with those in *S. pneumoniae*-infected mice (Fig. 2A and B, middle). Similarly, bacterial loads at 6 h and 12 h after pneumococcal infection at 28 dpi were both significantly decreased in the lungs of dually infected mice compared with *S. pneumoniae*-infected mice (Fig. 2A and B, right).

Markedly improved lung lesions with reduced inflammatory infiltrates were observed in the lungs of dually infected mice compared with *S. pneumoniae*-infected mice at 6 h after pneumococcal infection at 14 dpi (Fig. 3A). In line with these observations, the percentage of lung areas affected was significantly decreased in dually infected mice compared with *S. pneumoniae*-infected mice at 6 h after pneumococcal infection at 14 dpi (Fig. 3B). Similar results were also observed at 6 h after pneumococcal infection at 28 dpi, though a statistical significance decrease in the percentage of lung areas affected in dually infected mice compared with *S. pneumoniae*-infected mice was not obtained (Fig. 3A and B).

The body weight changes and survival were also monitored after a $0.6 \times$ median lethal dose (1×10^8 CFU) of *S. pneumoniae* infection at 14 dpi. Weight loss was significantly reduced 1 day after pneumococcal infection in dually infected mice compared with *S. pneumoniae*-infected mice (Fig. 4C). The survival after pneumococcal infection was not different between dually infected mice and *S. pneumoniae*-infected mice (Fig. 4D). Collectively, the above results demonstrated that prior H9N2 virus infection increased pulmonary pneumococcal clearance and reduced pneumococcal pneumonia-induced morbidity in BALB/c mice after recovery from influenza.

H9N2 virus infection modulated pulmonary chemokine and cytokine responses to subsequent pneumococcal infection. To determine the pulmonary chemokine and cytokine responses to secondary pneumococcal infection following H9N2 virus infection, we measured the levels of chemokines (keratinocyte chemoattractant [KC] and mouse macrophage inflammatory protein-2 [MIP-2]), the anti-inflammatory cytokine

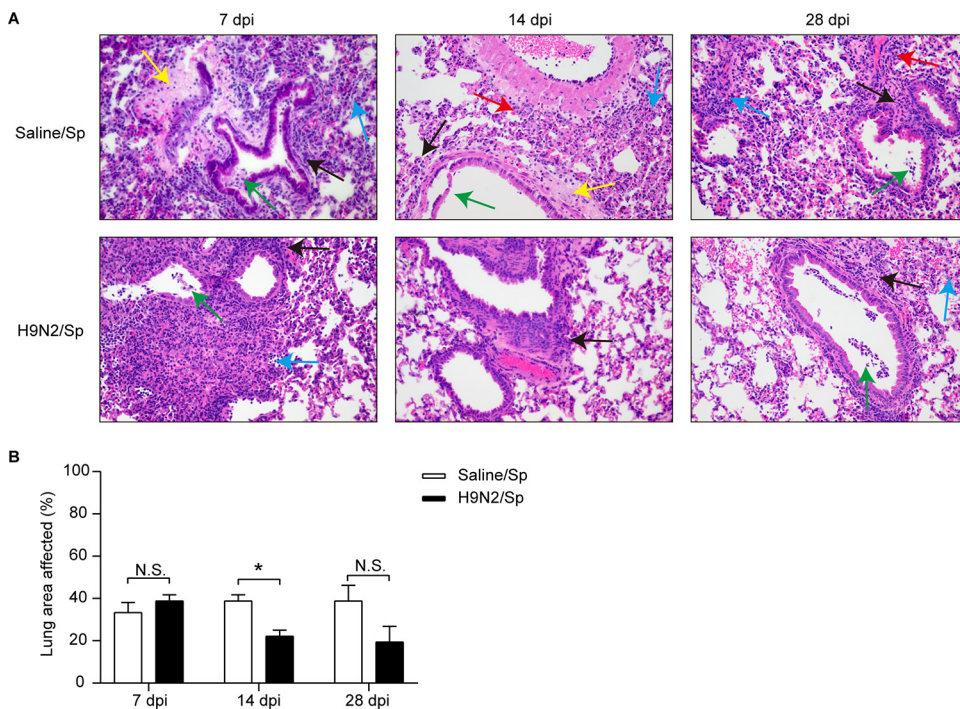


FIG 3 H9N2 virus infection alleviated pulmonary histopathological changes induced by pneumococcal infection at 14 dpi in BALB/c mice. (A) Representative H&E-stained lung sections (magnification, $\times 400$) of *S. pneumoniae*-infected mice and dually infected mice at 6 h after pneumococcal infection at 7, 14, or 28 dpi ($n=3$ /group). Denuded epithelia (green arrows), intra-alveolar fibrin exudation (yellow arrows), and extensive inflammatory cell recruitment around bronchioles (black arrows), alveoli (blue arrows), and blood vessels (red arrows) were observed at 6 h after pneumococcal infection. (B) Percentage of lung areas affected in *S. pneumoniae*-infected mice and dually infected mice, calculated from specified histopathological parameters, including peribronchial inflammation, intra-alveolar inflammation, perivascular inflammation, bronchial epithelial shedding, and intra-alveolar fibrin exudation ($n=3$ /group). Data are means and SEM. Two-tailed unpaired Student's *t* test was applied for two-group comparisons. *, $P < 0.05$; N.S., not significant. Sp, *Streptococcus pneumoniae*.

interleukin-10 (IL-10), and proinflammatory cytokines (IL-6, tumor necrosis factor alpha [TNF- α], and IL-1 β) at 6 h after pneumococcal infection at 7, 14, or 28 dpi.

After pneumococcal infection at 7 dpi, the levels of KC and MIP-2 were similar in the lungs of dually infected mice and *S. pneumoniae*-infected mice (Fig. 5A and B, left). The levels of IL-10, IL-6, and IL-1 β were also similar in the lungs of dually infected mice and *S. pneumoniae*-infected mice (Fig. 6A, B, and D, left). However, the TNF- α levels were significantly decreased in the lungs of dually infected mice compared with *S. pneumoniae*-infected mice (Fig. 6C, left). These data showed that H9N2 virus infection reduced TNF- α production after pneumococcal infection at 7 dpi.

After pneumococcal infection at 14 dpi, the levels of KC and MIP-2 were both significantly decreased in the lungs of dually infected mice compared with *S. pneumoniae*-infected mice (Fig. 5A and B, middle). The levels of IL-10, IL-6, and TNF- α were similar in the lungs of dually infected mice and *S. pneumoniae*-infected mice (Fig. 6A to C, middle). However, the IL-1 β levels were significantly increased in the lungs of dually infected mice compared with *S. pneumoniae*-infected mice (Fig. 6D, middle). After pneumococcal infection at 28 dpi, no statistically significant differences were found in the levels of these chemokines and cytokines between dually infected mice and *S. pneumoniae*-infected mice (Fig. 5A and B and 6A to D, right). Taken together, these results suggested that H9N2 virus infection reduced production of KC and MIP-2 but promoted IL-1 β production after pneumococcal infection at 14 dpi.

A high dose of H9N2 virus infection also promoted pulmonary pneumococcal clearance. Different doses of H9N2 virus infection might have different effects on the ability of the lung to clear *S. pneumoniae*. Therefore, we measured the bacterial loads at 12 h after pneumococcal infection following a low dose (6×10^4 PFU) or a high dose

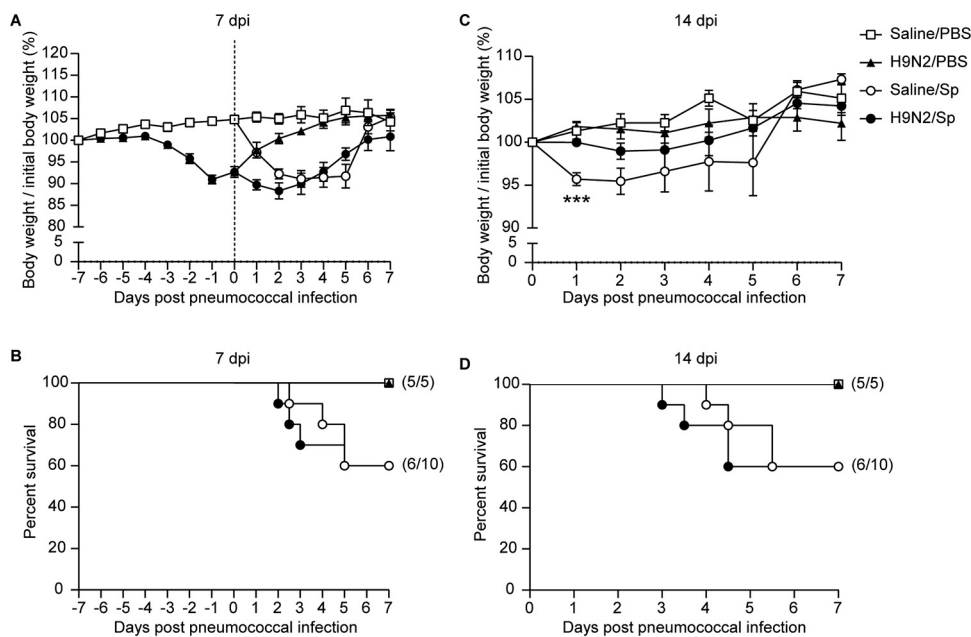


FIG 4 H9N2 virus infection did not change survival but reduced weight loss after secondary pneumococcal infection at 14 dpi in BALB/c mice. BALB/c mice were intranasally inoculated with 1.2×10^5 PFU of H9N2 virus or with noninfectious allantoic fluid diluted in sterile saline as a control; 7 or 14 days after H9N2 virus infection, mice were intranasally inoculated with a $0.6 \times$ median lethal dose (1×10^8 CFU) of *S. pneumoniae*. Body weight changes (A and C) and survival (B and D) after pneumococcal infection at 7 dpi (A and B) or 14 dpi (C and D) are shown (mock-infected mice and H9N2-infected mice, $n=5$ /group; *S. pneumoniae*-infected mice and dually infected mice, $n=10$ /group). Data are means and SEM. Two-tailed unpaired Student's *t* test was applied for body weight changes of two-group comparison, and a log-rank (Mantel-Cox) test was applied for survival comparison. ***, $P < 0.001$. PBS, phosphate-buffered saline; Sp, *Streptococcus pneumoniae*.

(1.2×10^6 PFU) of H9N2 virus. The significantly decreased bacterial loads at 12 h after pneumococcal infection at 14 dpi were also observed when mice were previously infected with the higher dose but not the lower dose, of H9N2 virus (Fig. 7). Thus, these data showed that the higher dose of H9N2 virus also promoted pulmonary pneumococcal clearance.

H9N2 virus infection increased pulmonary pneumococcal clearance in C57BL/6 mice after recovery from influenza. Previous studies have shown that BALB/c mice and C57BL/6 mice differ in their susceptibility to pneumococcal infection (36, 37). To determine whether the effect of H9N2 virus infection on pulmonary pneumococcal clearance was mouse strain specific, we measured the bacterial loads at 6 h after pneumococcal infection following H9N2 virus infection in C57BL/6 mice. Bacterial loads were similar in the lungs of dually infected mice and *S. pneumoniae*-infected mice after pneumococcal infection at 7 dpi (Fig. 8). In addition, bacterial loads showed a tendency to decrease in the lungs of dually infected mice compared with *S. pneumoniae*-infected mice after pneumococcal infection at 14 dpi, though this difference did not achieve statistical significance (Fig. 8). Further, bacterial loads were significantly decreased in the lungs of dually infected mice compared with *S. pneumoniae*-infected mice after

TABLE 1 Weight loss after secondary pneumococcal infection at 7 days after H9N2 virus infection

Group	% weight loss on day after pneumococcal infection ^a						
	1	2	3	4	5	6	7
<i>S. pneumoniae</i> -infected mice	8.18	12.76	14.81	13.69	15.20	3.28	-1.04
Dually infected mice	8.03	12.08	12.20	11.41	8.48	5.47	4.89

^aCalculated as mean percent of body weight in mock-infected mice - mean percent of body weight in *S. pneumoniae*-infected mice or mean percent of body weight in H9N2-infected mice - mean percent of body weight in dually infected mice.

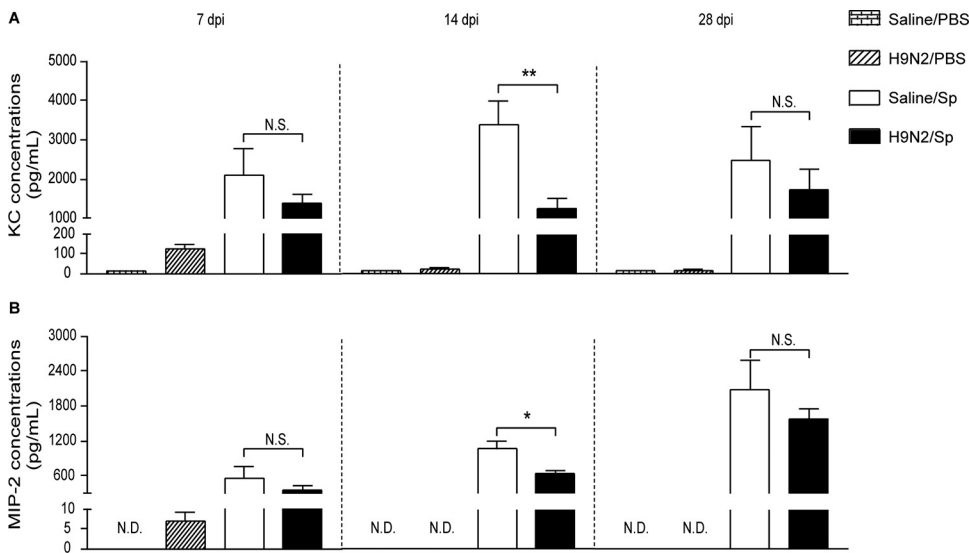


FIG 5 H9N2 virus infection reduced productions of KC and MIP-2 after pneumococcal infection at 14 dpi. Concentrations of (A) KC and (B) MIP-2 in the lungs of mock-infected mice, H9N2-infected mice, *S. pneumoniae*-infected mice, and dually infected mice at 6 h after pneumococcal infection at 7 dpi (left), 14 dpi (middle), or 28 dpi (right) ($n=3$ to 5/group). Data are means and SEM. Two-tailed unpaired Student's *t* test was applied for two-group comparisons. *, $P < 0.05$; **, $P < 0.01$; N.S., not significant. N.D., not detectable; KC, keratinocyte chemoattractant; MIP-2, mouse macrophage inflammatory protein-2; PBS, phosphate-buffered saline; Sp, *Streptococcus pneumoniae*.

pneumococcal infection at 21 dpi (Fig. 8). Similar results were obtained after pneumococcal infection at 28 and 35 dpi but not at 42 dpi (Fig. 8). Therefore, these results showed that H9N2 virus infection also increased pulmonary pneumococcal clearance in C57BL/6 mice after recovery from influenza.

DISCUSSION

H9N2 virus has been considered a potential pandemic strain due to its wide prevalence, extended range of mammalian hosts, and extensive genetic reassortment (13). Our results showed that a nonlethal dose (1.2×10^5 PFU) of H9N2 virus infection caused obvious signs of illness and significantly decreased body weight from 3 to 7 dpi in BALB/c mice. The virus was detected in the lungs of H9N2-infected mice at 3 and 7 dpi, and extensive inflammatory cellular infiltration was observed in the lungs of H9N2-infected mice at 7 dpi. Further, there were no significant differences between the H9N2-infected mice and mock-infected mice concerning the clinical signs and body weight at 14 dpi. The virus had been completely eliminated from the lungs of H9N2-infected mice by 14 dpi, and lung histopathology in H9N2-infected mice was similar to that in mock-infected mice at 14 dpi. These results showed that H9N2 virus infection caused obvious respiratory diseases in BALB/c mice and mice infected with H9N2 virus had recovered by 14 dpi, which was consistent with our previous and other published research findings (38–40).

Although influenza virus alone can have a substantial impact on global health, secondary bacterial infections postinfluenza are associated with increased morbidity and mortality during both epidemic and pandemic influenza outbreaks (23). Secondary bacterial pneumonia, particularly due to *S. pneumoniae*, accounted for more than 95% and 50% of severe illnesses and deaths that occurred during the 1918 pandemic and 2009 pandemic, respectively (17–20). Therefore, it is important to understand the interactions among influenza virus, host, and bacteria. Most previous studies utilizing mouse models showed that influenza virus infections could increase host susceptibility to secondary bacterial infections around 7 days postinfluenza by decreasing lung defense (29, 30, 41). Results from the study by Chockalingam et al. showed that H9N2 virus (A/Duck/Hong Kong/702/1979) infection increased susceptibility of BALB/c mice

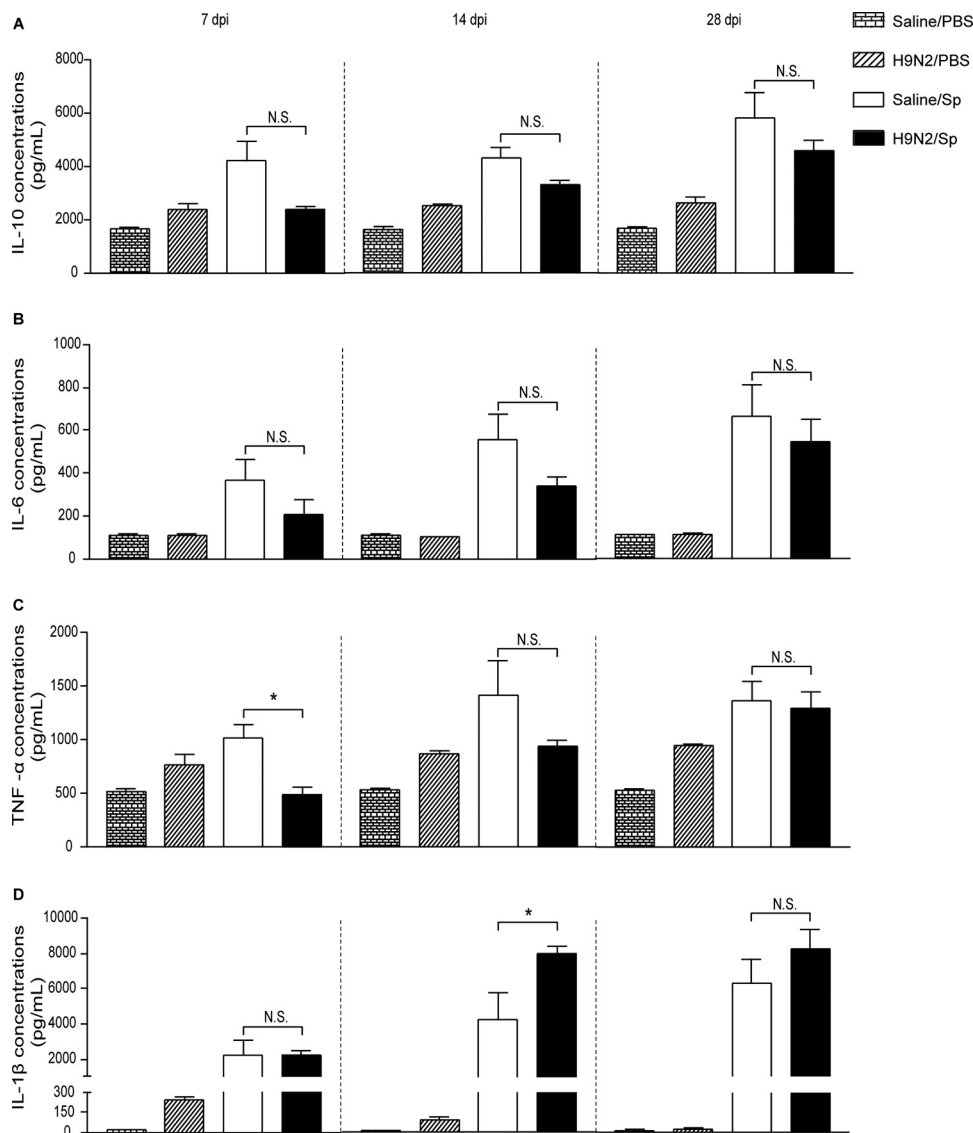


FIG 6 H9N2 virus infection reduced TNF- α production after pneumococcal infection at 7 dpi and promoted IL-1 β production after pneumococcal infection at 14 dpi. Concentrations of (A) IL-10, (B) IL-6, (C) TNF- α , and (D) IL-1 β in the lungs of mock-infected mice, H9N2-infected mice, *S. pneumoniae*-infected mice, and dually infected mice at 6 h after pneumococcal infection at 7 dpi (left), 14 dpi (middle), or 28 dpi (right) ($n=3$ to 5/group). Data are means and SEM. Two-tailed unpaired Student's *t* test was applied for two-group comparisons. *, $P < 0.05$; N.S., not significant. IL-10, interleukin-10; IL-6, interleukin-6; TNF- α , tumor necrosis factor alpha; IL-1 β , interleukin-1 β ; PBS, phosphate-buffered saline; Sp, *Streptococcus pneumoniae*.

to secondary pneumococcal infection at 7 days postinfluenza in terms of pulmonary bacterial loads, degree of weight loss, and survival (42). However, our results revealed that H9N2 virus (A/Chicken/Hebei/4/2008) infection did not increase the susceptibility of BALB/c mice to secondary pneumococcal infection at 7 dpi with respect to bacterial loads, lung histopathology, degree of weight loss, and survival. The disparate results between the study by Chockalingam et al. (42) and the present study might be due to the different strains of H9N2 virus being used. It has been proposed that several virulence factors of influenza virus have viral-strain-specific effects on the host that contribute to secondary bacterial pneumonia (43). Influenza viruses with functional PB1-F2 proteins or decreased glycosylation of surface proteins are thought to effectively facilitate subsequent bacterial infections (23). Additionally, high-activity neuraminidase of influenza viruses could cleave sialic acid receptors more effectively to expose bacterial

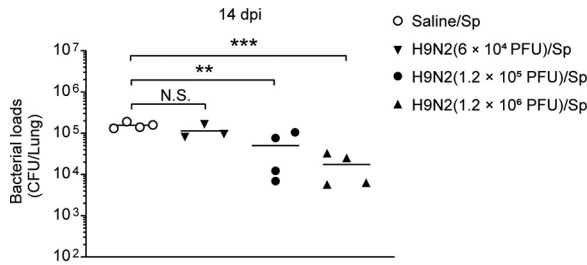


FIG 7 A high dose of H9N2 virus infection also promoted pulmonary pneumococcal clearance. BALB/c mice were intranasally inoculated with 6×10^4 PFU (low dose), 1.2×10^5 PFU, or 1.2×10^6 PFU (high dose) of H9N2 virus or with noninfectious allantoic fluid diluted in sterile saline as a control; 14 days after H9N2 virus infection, all mice were intranasally inoculated with 1×10^6 CFU of *S. pneumoniae*. Pulmonary bacterial loads at 12 h after pneumococcal infection were measured ($n=3$ or 4/group). Data are means and SEM. Ordinary one-way ANOVA followed by Tukey's multiple-comparison test was applied for four-group comparisons. **, $P < 0.01$; ***, $P < 0.001$; N.S., not significant. Sp, *Streptococcus pneumoniae*.

attachment receptors and enable bacteria to cause disease (41, 44). Results from the study of Peltola et al. showed that the neuraminidase activity of H9N2 virus from chicken was very low (44), which may help explain the fact that H9N2 virus (isolated from chicken) infection did not promote secondary pneumococcal infection at 7 dpi in our study.

Increased susceptibility of mice to secondary pneumococcal infection was also observed when mice were challenged with *S. pneumoniae* after recovery from influenza in numerous previous studies. For example, H1N1 and H3N2 virus infection was shown to cause significantly increased pulmonary bacterial loads and mortality after pneumococcal infection at 14 days postinfluenza in mice (45–48). In addition, a study performed by Didierlaurent et al. demonstrated that H3N2 virus infection could still lead to significantly increased pulmonary bacterial loads and mortality after pneumococcal infection at 42 days postinfluenza in mice (46). In contrast, our results showed that H9N2 virus infection caused significantly decreased bacterial loads after pneumococcal infection at 14 or 28 dpi, suggesting that prior H9N2 virus infection increased pulmonary pneumococcal clearance in mice after recovery from influenza. Consistent with decreased bacterial loads, markedly alleviated pulmonary histopathological changes were also observed after pneumococcal infection at 14 dpi. In addition, H9N2 virus infection led to significantly reduced weight loss but did not change the mortality after pneumococcal infection at 14 dpi. These results implied that the effect of H9N2 virus infection on increasing the host resistance to pneumococcal infection at 14 dpi is limited; i.e., it could reduce secondary pneumococcal pneumonia-induced morbidity but was not sufficient to decrease secondary pneumococcal pneumonia-induced mortality in BALB/c mice.

We also determined whether the dose of H9N2 virus impacts the pulmonary pneumococcal clearance. Our result showed that the significantly decreased bacterial loads

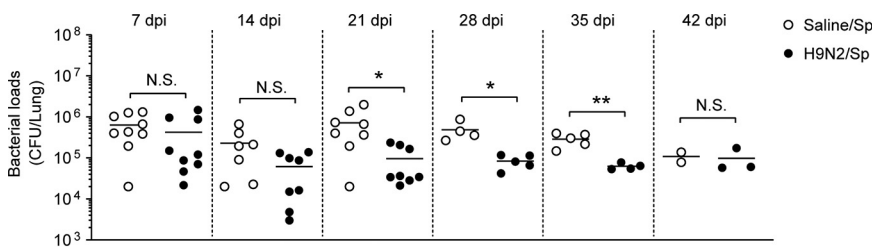


FIG 8 H9N2 virus infection increased pulmonary pneumococcal clearance in C57BL/6 mice when secondary pneumococcal infection was performed at 21, 28, or 35 dpi. C57BL/6 mice were intranasally inoculated with 1.2×10^5 PFU of H9N2 virus or with noninfectious allantoic fluid diluted in sterile saline as a control; 7, 14, 21, 28, 35, 42 days after H9N2 virus infection, mice were intranasally inoculated after with 1×10^6 CFU of *S. pneumoniae*. Pulmonary bacterial loads at 6 h after pneumococcal infection were measured ($n=2$ to 9/group). Data are means and SEM. Two-tailed unpaired Student's *t* test were applied for two-group comparisons: *, $P < 0.05$; **, $P < 0.01$; N.S., not significant. Sp, *Streptococcus pneumoniae*.

after pneumococcal infection were also observed when mice were infected 14 days previously with a high dose but not a low dose of H9N2 virus. Thus, the higher dose of H9N2 virus also promoted pulmonary pneumococcal clearance. Moreover, the beneficial effect of H9N2 virus infection on pulmonary pneumococcal clearance was not dependent on active viral replication, as the virus had been completely eliminated from the lungs of H9N2-infected mice by 14 dpi.

It has been reported that C57BL/6 mice are more susceptible to pneumococcal infection than BALB/c mice (36, 37). In the present study, our results showed that, similar to the results obtained in BALB/c mice, H9N2 virus infection led to significantly decreased bacterial loads after pneumococcal infection at 21, 28, and 35 dpi in C57BL/6 mice, suggesting that the beneficial effect of H9N2 virus infection on pulmonary pneumococcal clearance was not mouse strain specific.

Recently, similar to our results, Aegerter et al. found that H3N2 virus preceding 28-day infection also increased host resistance to secondary pneumococcal infection in terms of bacterial loads and mortality in C57BL/6 mice, and this prolonged antibacterial protection was attributed to a population of monocyte-derived alveolar macrophages that produce increased IL-6 (49). During pneumococcal infection, neutrophils also play a key role in eliminating *S. pneumoniae* (50). The exact roles of macrophages and neutrophils underlying the protection against secondary pneumococcal infection conferred by H9N2 virus infection would need to be investigated in further studies.

It is generally assumed that local production of chemokines and cytokines, as an important part of the innate immune response against bacterial infections, might play a role in the clearance of bacterial pathogens. However, a study done by Dallaire et al. showed that the levels of KC, MIP-2, IL-6, and IL-1 β in lungs of mice with pneumococcal infection were positively correlated with bacterial load (51). It was also shown that the production of KC, IL-10, IL-6, TNF- α , and IL-1 β was significantly enhanced when bacterial loads were also significantly increased after *S. pneumoniae* infection at 7 days after H9N2 virus (A/Duck/Hong Kong/702/1979) infection (42). Our results showed that the production of KC, MIP-2, IL-10, IL-6, and IL-1 β did not significantly change when bacterial loads were similar in the lungs of dually infected mice and *S. pneumoniae*-infected mice after pneumococcal infection at 7 dpi. These results might be explained by the fact that production of these mediators is dependent, at least in part, on direct stimulation by *S. pneumoniae*. However, TNF- α production was significantly reduced in the lungs of dually infected mice compared with *S. pneumoniae*-infected mice when bacterial loads were similar between the two groups after pneumococcal infection at 7 dpi in our study. Results from the study of Kirby et al. showed that TNF- α was produced mainly by alveolar macrophages during pneumococcal pneumonia but was not essential for pneumococcal clearance (52). Thus, the significantly decreased TNF- α production in the present study might be explained by the fact that H9N2 virus preceding 7-day infection limited the ability of alveolar macrophages to produce TNF- α without impacting pneumococcal clearance.

When secondary pneumococcal infections were performed at 14 dpi, the production of KC and MIP-2 was significantly reduced when bacterial loads were significantly decreased in the lungs of dually infected mice compared with *S. pneumoniae*-infected mice in our study. Conversely, KC production was significantly enhanced when bacterial loads were significantly increased after pneumococcal infection at 14 days after H1N1 infection or at 14 days after H3N2 infection (47, 48). These results also suggested that production of KC and MIP-2 after secondary pneumococcal infection at 14 days after influenza was associated with the direct stimulation by *S. pneumoniae*. In addition, the production of IL-10, IL-6, and TNF- α did not significantly change, notably in contrast to IL-1 β , which was significantly enhanced after pneumococcal infection at 14 dpi in our study. Recently, enhanced IL-1 β production was shown to be associated with induction of trained immunity (53–55). The concept of trained immunity is proposed to describe the fact that long-term activation of innate immune responses by certain pathogens or live vaccines could confer nonspecific protection against subsequent

infections by dissimilar pathogens (56). Taking this into account, the beneficial effect of H9N2 virus infection on pulmonary pneumococcal clearance might partially be due to the induction of trained immunity associated with the enhanced IL-1 β production. Since bacterial loads were significantly decreased but IL-1 β production did not significantly change after pneumococcal infection at 28 dpi, other cellular and soluble mediators might be involved in improving bacterial clearance during secondary pneumococcal infection following resolution of H9N2 virus infection. Further investigation would be required to clarify the induction of trained immunity by H9N2 virus infection.

In conclusion, our study shows that H9N2 virus infection did not enhance the susceptibility of mice to secondary pneumococcal infection at 7 days after H9N2 virus infection, and increased pulmonary pneumococcal clearance was seen upon secondary pneumococcal infection after resolution of H9N2 virus infection. The interactions among influenza virus, host, and *S. pneumoniae* are complex, and the effects of other influenza virus infections on susceptibility to secondary pneumococcal infection need to be investigated in further studies.

MATERIALS AND METHODS

Mouse strains. Specific-pathogen-free (SPF) male BALB/c mice and C57BL/6 mice, all of which were between 6 and 8 weeks of age and weighed 18 to 20 g, were purchased from Beijing Vital River Laboratory Animal Technology Company Limited (China). All mouse experiments were approved by the Laboratory Animal Welfare and Animal Experimental Ethical Committee of China Agricultural University (no. AW12210202-2). All mice were acclimatized for 7 days before experimental treatments and had free access to food and water during the experiments.

Viral and bacterial strains. The H9N2 virus [A/Chicken/Hebei/4/2008(H9N2)] used in this study is one of the representative H9N2 isolates in northern China (57). The complete genome sequences of the virus are available in GenBank under accession numbers [FJ499463](#) to [FJ499470](#). Its pathogenicity in mice was assessed in detail in our previous study, and the results showed that this H9N2 virus infection caused severe lung injury with a high mortality without prior adaptation (38). The virus was propagated in the allantoic cavities of 10-day-old embryonated SPF chicken eggs at 37°C for 72 h, and then the allantoic fluid was centrifuged and stored at -80°C for use in all of the experiments described herein. For H9N2 viral inoculation, the frozen virus liquid was thawed and diluted in sterile saline. Actual H9N2 virus concentration was determined by plaque assay as described below. Results were expressed as PFU per milliliter.

S. pneumoniae (NCTC7466, serotype 2) was grown in Todd-Hewitt broth supplemented with 0.5% yeast extract broth at 37°C. When cultured at mid-log phase (optical density at 600 nm [OD₆₀₀]=0.3 to 0.4), the pneumococcal culture maintained in broth plus 20% glycerol was stored at -80°C for use in all of the experiments described herein (58). For *S. pneumoniae* inoculation, the frozen stock was thawed and cultured in broth at 37°C until mid-logarithmic phase. Then the culture was centrifuged, washed twice in sterile phosphate-buffered saline (PBS), and subsequently pelleted before dilution to the desired concentration. Actual pneumococcal concentration was determined by plating 0.1 ml of 10-fold serial dilutions on blood agar plates, and colonies were counted after incubation for 24 h at 37°C. Results were expressed as CFU per milliliter.

Viral and bacterial inoculation. Mice were lightly anesthetized by inhalation of isoflurane and then received a volume of 50 μ l of viral or bacterial suspension at the tip of the nose, which was involuntarily inhaled. To facilitate the migration of the inoculum to the lung, mice were held in an upright position for 1 min. As a control, mice were mock infected with 50 μ l of noninfectious allantoic fluid or sterile PBS in an identical manner.

Experimental protocol. The present study was designed to observe the effect of H9N2 virus infection on host resistance to secondary pneumococcal infection at different time points after H9N2 virus infection (Fig. 9) and was performed in three parts, as follows.

In the first part, two experiments were carried out. The first experiment was to observe the effect of H9N2 virus infection on the bacterial loads, lung histopathology, and cytokine levels after pneumococcal infection. BALB/c mice were intranasally inoculated with 1.2×10^5 PFU of H9N2 virus or with noninfectious allantoic fluid as a control. Seven, 14, or 28 days after H9N2 virus infection, mice were intranasally inoculated with 1×10^6 CFU of *S. pneumoniae* or with sterile PBS as a control (experimental mouse groups are shown in Table 2). The dose of 1.2×10^5 PFU of H9N2 virus was chosen, as a pilot experiment had indicated that mice infected with 1.2×10^5 PFU of H9N2 viruses would be ill but not dead and could be used to conduct secondary pneumococcal inoculation after H9N2 virus infection. After H9N2 virus infection, clinical signs and body weight, as measures of morbidity, were monitored daily; viral titers were measured at 3, 7, 14, and 28 dpi, and lung histopathology was assessed at 7, 14, and 28 dpi in mock-infected mice and H9N2-infected mice. After pneumococcal infection at 7, 14, or 28 dpi, the four groups of mice were sacrificed at 6 h or 12 h, and the whole lung tissues were harvested to analyze the lung histopathology, bacterial loads, and cytokine levels as described below.

The second experiment was to observe the effect of H9N2 virus infection on the body weight changes and survival after pneumococcal infection. BALB/c mice were also randomized into four groups as described in Table 2. H9N2 virus infection was performed as described for the first experiment, and

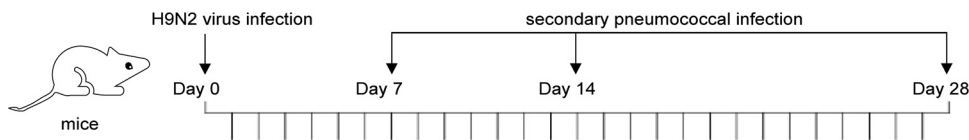


FIG 9 Schematic diagram of H9N2 virus infection and secondary pneumococcal infection. Secondary pneumococcal infections were mainly performed at 7, 14, or 28 days after H9N2 virus infection in mice.

secondary pneumococcal infection was performed by intranasally inoculating mice with a $0.6 \times$ median lethal dose (1×10^8 CFU) of *S. pneumoniae* at 7 or 14 dpi. Body weight was monitored daily, and survival was recorded every 12 h until 7 days after pneumococcal infection, when no more deaths were observed. Mice were euthanized when they had lost over 25% of their initial weight and appeared moribund (based on inability to move freely and access food and water) and were considered to have died on that day (42).

In the second part, we determined whether the dose of H9N2 virus impacts the pulmonary pneumococcal clearance. BALB/c mice were intranasally inoculated with 6×10^4 PFU (low dose), 1.2×10^5 PFU, or 1.2×10^6 PFU (high dose) of H9N2 virus, and then all were intranasally inoculated with 1×10^6 CFU of *S. pneumoniae* at 14 dpi. The mice were sacrificed at 12 h after pneumococcal infection and the whole lung tissues were harvested to analyze the bacterial load as described below.

In the third part, we determine whether the effect of H9N2 virus infection on pulmonary pneumococcal clearance was mouse strain specific, as previous studies have shown that BALB/c mice and C57BL/6 mice differ in their susceptibility to pneumococcal infection (36, 37). C57BL/6 mice were intranasally inoculated with 1.2×10^5 PFU of H9N2 virus and then intranasally inoculated with 1×10^6 CFU of *S. pneumoniae* at 7, 14, 21, 28, 35, or 42 dpi. The mice were sacrificed at 6 h after pneumococcal infection, and whole lung tissues were harvested to analyze the bacterial load as described below.

Plaque assay. At the indicated time points after H9N2 virus inoculation, mice were sacrificed by cervical dislocation, and the whole lungs were collected aseptically in sterile tubes and homogenized in 1 ml of sterile saline. The lung homogenates were centrifuged, and then the supernatants were filtered using a $0.22\text{-}\mu\text{m}$ filter membrane. Then, H9N2 virus concentrations in lung tissues were determined by plaque assay as described previously (59). Briefly, adsorption of 0.5 ml of 10-fold serial dilutions of viral samples was performed on Madin-Darby canine kidney monolayers, which were overlaid with a 1% final concentration of agarose and a $1\ \mu\text{g/ml}$ final concentration of TPCK (tosylsulfonil phenylalanyl chloromethyl ketone) trypsin. After 72 h, cells were fixed with 4% formaldehyde and stained with 2% crystal violet to detect plaques. Viral titer (in PFU per milliliter) was calculated as plaque counts/(0.5 ml \times dilution factor of the sample).

Histopathological examination of lung tissues. At the indicated time points after H9N2 virus or *S. pneumoniae* inoculation, the left lobes of the lungs were removed immediately after euthanasia, fixed in 4% paraformaldehyde, and then embedded in paraffin. Fixed sections (3 to $5\ \mu\text{m}$) of paraffin-embedded lungs were stained with hematoxylin-eosin (H&E) for examining histopathological alterations in the lung parenchyma under a light microscope. Based on the extent of histopathological alterations, including peribronchial inflammation, intra-alveolar inflammation, perivascular inflammation, bronchial epithelial shedding, and intra-alveolar fibrin exudation, three sections per lung were blindly scored on a scale of 0 (no lung area affected) to 4 (100% of the lung area affected) by an experienced pathologist, as described previously (60, 61). Results were expressed as percentage of lung area affected, calculated as (total scores of three sections/3) \times 25%.

Measurement of bacterial loads in lung tissues. At the indicated time points after *S. pneumoniae* inoculation, mice were sacrificed by cervical dislocation, and the whole lungs were collected aseptically in sterile tubes and homogenized in 1 ml of sterile PBS. Then the volume of the lung homogenate was increased to 3 ml with sterile PBS. Finally, bacterial loads in lung tissues were determined by plating 0.1 ml of 10-fold serial dilutions on blood agar plates, and colonies were counted after incubating for 24 h at 37°C . Bacterial loads (CFU per lung) were calculated as (colony counts \times 3 ml)/(0.1 ml \times dilution factor of the sample) (58).

Measurement of cytokine levels in lung tissues. Lung homogenates were centrifuged and the supernatants were collected and stored at -80°C until measurement of cytokine levels. The levels of keratinocyte chemoattractant (KC), mouse macrophage inflammatory protein-2 (MIP-2), and interleukin-1 β (IL-1 β) were measured using mouse Quantikine enzyme-linked immunosorbent assay (ELISA) kits (R&D Systems, USA). The levels of interleukin-6 (IL-6), tumor necrosis factor alpha (TNF- α), and interleukin-10

TABLE 2 Experimental mouse groups after secondary pneumococcal infection

Group	Primary inoculation	Secondary inoculation
Mock infected	Noninfectious allantoic fluid	Sterile PBS
H9N2 infected	H9N2 virus	Sterile PBS
<i>S. pneumoniae</i> infected	Noninfectious allantoic fluid	<i>S. pneumoniae</i>
Dually infected	H9N2 virus	<i>S. pneumoniae</i>

(IL-10) were measured using mouse Quantikine ELISA kits (Solarbio, China). All of the above-mentioned cytokines were measured according to the manufacturer's instructions.

Statistical analysis. All data are presented as means and standard errors of the means (SEM). Data between two groups were analyzed by using two-tailed unpaired Student's *t* test. Data among multiple groups were analyzed by using ordinary one-way analysis of variance (ANOVA) followed by Tukey's multiple-comparison test. Survival data were analyzed by using a log-rank (Mantel-Cox) test. All statistical analyses were performed using GraphPad Prism 8 software (GraphPad Software, USA). Results with *P* values of <0.05 were considered significant.

ACKNOWLEDGMENTS

We thank Xuemei Zhang (Department of Laboratory Medicine, Chongqing Medical University, Chongqing, China) for providing *S. pneumoniae* (NCTC 7466).

This work was supported by the national key research and development program Study on Nutrition Metabolism and Prevention and Control Technology of Toxic Diseases of Livestock and Poultry (no. 2016YFD0501200) and Earmarked Fund for Layer and Broiler Innovation Team of the Second Phase of Hebei Modern Industrial System (HBCT2018150101 and HBCT2018150207).

Jingyun Li designed and performed most of the experiments, analyzed data, and wrote the article. Hongyan Wang, Pengjing Lian, Yu Bai, Zihui Zhang, Lihong Zhao, and Tong Xu helped perform experiments. Jian Qiao conceived the project, analyzed data, and revised the article. All authors read and approved the final article.

We declare no conflict of interest.

REFERENCES

- Nagy A, Mettenleiter TC, Abdelwhab EM. 2017. A brief summary of the epidemiology and genetic relatedness of avian influenza H9N2 virus in birds and mammals in the Middle East and North Africa. *Epidemiol Infect* 145:3320–3333. <https://doi.org/10.1017/S0950268817002576>.
- Bi Y, Li J, Li S, Fu G, Jin T, Zhang C, Yang Y, Ma Z, Tian W, Li J, Xiao S, Li L, Yin R, Zhang Y, Wang L, Qin Y, Yao Z, Meng F, Hu D, Li D, Wong G, Liu F, Lv N, Wang L, Fu L, Yang Y, Peng Y, Ma J, Sharshov K, Shestopalov A, Gulyaeva M, Gao GF, Chen J, Shi Y, Liu WJ, Chu D, Huang Y, Liu Y, Liu L, Liu W, Chen Q, Shi W. 2020. Dominant subtype switch in avian influenza viruses during 2016–2019 in China. *Nat Commun* 11:5909. <https://doi.org/10.1038/s41467-020-19671-3>.
- Wang J, Wu M, Hong W, Fan X, Chen R, Zheng Z, Zeng Y, Huang R, Zhang Y, Lam TT, Smith DK, Zhu H, Guan Y. 2016. Infectivity and transmissibility of avian H9N2 influenza viruses in pigs. *J Virol* 90:3506–3514. <https://doi.org/10.1128/JVI.02605-15>.
- Zhang C, Xuan Y, Shan H, Yang H, Wang J, Wang K, Li G, Qiao J. 2015. Avian influenza virus H9N2 infections in farmed minks. *Virol J* 12:180. <https://doi.org/10.1186/s12985-015-0411-4>.
- Huang Y, Li X, Zhang H, Chen B, Jiang Y, Yang L, Zhu W, Hu S, Zhou S, Tang Y, Xiang X, Li F, Li W, Gao L. 2015. Human infection with an avian influenza A (H9N2) virus in the middle region of China. *J Med Virol* 87:1641–1648. <https://doi.org/10.1002/jmv.24231>.
- Chen Y, Ge W, Huang C, Lai Z, Fan X. 2008. Serological survey of antibody to H9 and H6 subtypes of bird flu virus in healthy youths in Guangxi. *China Tropical Medicine* 6:985–986. (In Chinese.)
- Liang Q, Li J, Chen Y, Xuan W, Ning J, Wei Y, Li K. 2003. Seroepidemiologic survey for antibody of healthy youth to H9, H6 and H5 subtypes of influenza A virus in chaoshan area. *J Shantou University Medical College* 2:107–108. (In Chinese.)
- Liu D, Shi W, Shi Y, Wang D, Xiao H, Li W, Bi Y, Wu Y, Li X, Yan J, Liu W, Zhao G, Yang W, Wang Y, Ma J, Shu Y, Lei F, Gao GF. 2013. Origin and diversity of novel avian influenza A H7N9 viruses causing human infection: phylogenetic, structural, and coalescent analyses. *Lancet* 381:1926–1932. [https://doi.org/10.1016/S0140-6736\(13\)60938-1](https://doi.org/10.1016/S0140-6736(13)60938-1).
- Pu J, Wang S, Yin Y, Zhang G, Carter RA, Wang J, Xu G, Sun H, Wang M, Wen C, Wei Y, Wang D, Zhu B, Lemmon G, Jiao Y, Duan S, Wang Q, Du Q, Sun M, Bao J, Sun Y, Zhao J, Zhang H, Wu G, Liu J, Webster RG. 2015. Evolution of the H9N2 influenza genotype that facilitated the genesis of the novel H7N9 virus. *Proc Natl Acad Sci U S A* 112:548–553. <https://doi.org/10.1073/pnas.1422456112>.
- Chen H, Yuan H, Gao R, Zhang J, Wang D, Xiong Y, Fan G, Yang F, Li X, Zhou J, Zou S, Yang L, Chen T, Dong L, Bo H, Zhao X, Zhang Y, Lan Y, Bai T, Dong J, Li Q, Wang S, Zhang Y, Li H, Gong T, Shi Y, Ni X, Li J, Zhou J, Fan J, Wu J, Zhou X, Hu M, Wan J, Yang W, Li D, Wu G, Feng Z, Gao GF, Wang Y, Jin Q, Liu M, Shu Y. 2014. Clinical and epidemiological characteristics of a fatal case of avian influenza A H10N8 virus infection: a descriptive study. *Lancet* 383:714–721. [https://doi.org/10.1016/S0140-6736\(14\)60111-2](https://doi.org/10.1016/S0140-6736(14)60111-2).
- Liu D, Shi WF, Gao GF. 2014. Poultry carrying H9N2 act as incubators for novel human avian influenza viruses. *Lancet* 383:869–869. [https://doi.org/10.1016/S0140-6736\(14\)60386-X](https://doi.org/10.1016/S0140-6736(14)60386-X).
- Bi Y, Chen Q, Wang Q, Chen J, Jin T, Wong G, Quan C, Liu J, Wu J, Yin R, Zhao L, Li M, Ding Z, Zou R, Xu W, Li H, Wang H, Tian K, Fu G, Huang Y, Shestopalov A, Li S, Xu B, Yu H, Luo T, Lu L, Xu X, Luo Y, Liu Y, Shi W, Liu D, Gao GF. 2016. Genesis, evolution and prevalence of H5N6 avian influenza viruses in China. *Cell Host Microbe* 20:810–821. <https://doi.org/10.1016/j.chom.2016.10.022>.
- Song W, Qin K. 2020. Human-infecting influenza A (H9N2) virus: a forgotten potential pandemic strain? *Zoonoses Public Health* 67:203–212. <https://doi.org/10.1111/zph.12685>.
- Adegbola RA, DeAntonio R, Hill PC, Roca A, Usuf E, Hoet B, Greenwood BM. 2014. Carriage of *Streptococcus pneumoniae* and other respiratory bacterial pathogens in low and lower-middle income countries: a systematic review and meta-analysis. *PLoS One* 9:e103293. <https://doi.org/10.1371/journal.pone.0103293>.
- Mackenzie GA, Leach AJ, Carapetis JR, Fisher J, Morris PS. 2010. Epidemiology of nasopharyngeal carriage of respiratory bacterial pathogens in children and adults: cross-sectional surveys in a population with high rates of pneumococcal disease. *BMC Infect Dis* 10:304. <https://doi.org/10.1186/1471-2334-10-304>.
- Troeger C, Blacker BF, Khalil IA, Rao PC, Cao SJ, Zimsen SRM, Albertson S, Stanaway JD, Deshpande A, Farag T, Forouzanfar MH, Abebe Z, Adetifa IMO, Adhikari TB, Akibu M, Al Lami FH, Al-Eyadhy A, Alvis-Guzman N, Amare AT, Amoako YA, Antonio CAT, Aremu O, Asfaw ET, Asgedom SW, Atey TM, Attia EF, Avokpaho EFGA, Ayele HT, Ayuk TB, Balakrishnan K, Barac A, Bassat Q, Behzadifar M, Behzadifar M, Bhaumik S, Bhutta ZA, Bijani A, Brauer M, Brown A, Camargos PAM, Castaneda-Orjuela CA, Colombara D, Conti S, Dadi AF, Dandona L, Dandona R, Do HP, Dubljanin E, Edessa D, Elkout H, et al. 2018. Estimates of the global, regional, and national morbidity, mortality, and aetiologies of lower respiratory infections in 195 countries, 1990–2016: a systematic analysis for the Global Burden of Disease Study 2016. *Lancet Infect Dis* 18:1191–1210. [https://doi.org/10.1016/S1473-3099\(18\)30310-4](https://doi.org/10.1016/S1473-3099(18)30310-4).
- Morens DM, Taubenberger JK, Fauci AS. 2008. Predominant role of bacterial pneumonia as a cause of death in pandemic influenza: implications for pandemic influenza preparedness. *J Infect Dis* 198:962–970. <https://doi.org/10.1086/591708>.

18. Brundage JF, Shanks GD. 2008. Deaths from bacterial pneumonia during 1918–19 influenza pandemic. *Emerg Infect Dis* 14:1193–1199. <https://doi.org/10.3201/eid1408.071313>.
19. Palacios G, Hornig M, Cisterna D, Savji N, Bussetti AV, Kapoor V, Hui J, Tokarz R, Briese T, Baumeister E, Lipkin WI. 2009. Streptococcus pneumoniae coinfection is correlated with the severity of H1N1 pandemic influenza. *PLoS One* 4:e8540. <https://doi.org/10.1371/journal.pone.0008540>.
20. Gill JR, Sheng ZM, Ely SF, Guinee DG, Beasley MB, Suh J, Deshpande C, Mollura DJ, Morens DM, Bray M, Travis WD, Taubenberger JK. 2010. Pulmonary pathologic findings of fatal 2009 pandemic influenza A/H1N1 viral infections. *Arch Pathol Lab Med* 134:235–243. <https://doi.org/10.1043/1543-2165-134.2.235>.
21. Weinberger DM, Harboe ZB, Viboud C, Krause TG, Miller M, Molbak K, Konradsen HB. 2014. Pneumococcal disease seasonality: incidence, severity and the role of influenza activity. *Eur Respir J* 43:833–841. <https://doi.org/10.1183/09031936.00056813>.
22. Wherry WB, Butterfield CT. 1920. Inhalation experiments on influenza and pneumonia and on the importance of spray-borne bacteria in respiratory infections. *J Infect Dis* 27:315–326. <https://doi.org/10.1093/infdis/27.4.315>.
23. McCullers JA. 2014. The co-pathogenesis of influenza viruses with bacteria in the lung. *Nat Rev Microbiol* 12:252–262. <https://doi.org/10.1038/nrmicro3231>.
24. McCullers JA, McAuley JL, Browall S, Iverson AR, Boyd KL, Henriques Normark B. 2010. Influenza enhances susceptibility to natural acquisition of and disease due to Streptococcus pneumoniae in ferrets. *J Infect Dis* 202:1287–1295. <https://doi.org/10.1086/656333>.
25. Pittet LA, Hall-Stoodley L, Rutkowski MR, Harmsen AG. 2010. Influenza virus infection decreases tracheal mucociliary velocity and clearance of Streptococcus pneumoniae. *Am J Respir Cell Mol Biol* 42:450–460. <https://doi.org/10.1165/rcmb.2007-0417OC>.
26. Plotkowski MC, Puchelle E, Beck G, Jacquot J, Hannoun C. 1986. Adherence of type I Streptococcus pneumoniae to tracheal epithelium of mice infected with influenza A/PR8 virus. *Am Rev Respir Dis* 134:1040–1044. <https://doi.org/10.1164/arrd.1986.134.5.1040>.
27. Li N, Ren A, Wang X, Fan X, Zhao Y, Gao GF, Cleary P, Wang B. 2015. Influenza viral neuraminidase primes bacterial coinfection through TGF-beta-mediated expression of host cell receptors. *Proc Natl Acad Sci U S A* 112:238–243. <https://doi.org/10.1073/pnas.1414422112>.
28. Jochems SP, Marcon F, Carniel BF, Holloway M, Mitsi E, Smith E, Gritzfeld JF, Solorzano C, Reine J, Pojar S, Nikolaou E, German EL, Hyder-Wright A, Hill H, Hales C, de Steenhuisen Piters WAA, Bogaert D, Adler H, Zaidi S, Connor V, Gordon SB, Rylance J, Nakaya HI, Ferreira DM. 2018. Inflammation induced by influenza virus impairs human innate immune control of pneumococcus. *Nat Immunol* 19:1299–1308. <https://doi.org/10.1038/s41590-018-0231-y>.
29. Ghoneim HE, Thomas PG, McCullers JA. 2013. Depletion of alveolar macrophages during influenza infection facilitates bacterial superinfections. *J Immunol* 191:1250–1259. <https://doi.org/10.4049/jimmunol.1300014>.
30. Sun K, Metzger DW. 2008. Inhibition of pulmonary antibacterial defense by interferon-gamma during recovery from influenza infection. *Nat Med* 14:558–564. <https://doi.org/10.1038/nm1765>.
31. Engelich G, White M, Hartshorn KL. 2001. Neutrophil survival is markedly reduced by incubation with influenza virus and Streptococcus pneumoniae: role of respiratory burst. *J Leukoc Biol* 69:50–56.
32. Schliehe C, Flynn EK, Vilagos B, Richson U, Swaminathan S, Bosnjak B, Bauer L, Kandasamy RK, Griesshammer IM, Kosack L, Schmitz F, Litvak V, Sissons J, Lercher A, Bhattacharya A, Khamina K, Trivett AL, Tessarollo L, Mesteri I, Hladik A, Merkler D, Kubicek S, Knapp S, Epstein MM, Symer DE, Aderem A, Bergthaler A. 2015. The methyltransferase Setdb2 mediates virus-induced susceptibility to bacterial superinfection. *Nat Immunol* 16:67–74. <https://doi.org/10.1038/ni.3046>.
33. Mehta D, Petes C, Gee K, Basta S. 2015. The role of virus infection in deregulating the cytokine response to secondary bacterial infection. *J Interferon Cytokine Res* 35:925–934. <https://doi.org/10.1089/jir.2015.0072>.
34. Cox NJ, Fukuda K. 1998. Influenza. *Infect Dis Clin North Am* 12:27–38. [https://doi.org/10.1016/s0891-5520\(05\)70406-2](https://doi.org/10.1016/s0891-5520(05)70406-2).
35. Smith AM, McCullers JA. 2014. Secondary bacterial infections in influenza virus infection pathogenesis. *Curr Top Microbiol Immunol* 385:327–356. https://doi.org/10.1007/82_2014_394.
36. Gingles NA, Alexander JE, Kadioglu A, Andrew PW, Kerr A, Mitchell TJ, Hopes E, Denny P, Brown S, Jones HB, Little S, Booth GC, McPheat WL. 2001. Role of genetic resistance in invasive pneumococcal infection: identification and study of susceptibility and resistance in inbred mouse strains. *Infect Immun* 69:426–434. <https://doi.org/10.1128/IAI.69.1.426-434.2001>.
37. Preston JA, Beagley KW, Gibson PG, Hansbro PM. 2004. Genetic background affects susceptibility in nonfatal pneumococcal bronchopneumonia. *Eur Respir J* 23:224–231. <https://doi.org/10.1183/09031936.03.00081403>.
38. Deng G, Bi J, Kong F, Li X, Xu Q, Dong J, Zhang M, Zhao L, Luan Z, Lv N, Qiao J. 2010. Acute respiratory distress syndrome induced by H9N2 virus in mice. *Arch Virol* 155:187–195. <https://doi.org/10.1007/s00705-009-0560-0>.
39. Gui B, Chen Q, Hu C, Zhu C, He G. 2017. Effects of calcitriol (1, 25-dihydroxy-vitamin D3) on the inflammatory response induced by H9N2 influenza virus infection in human lung A549 epithelial cells and in mice. *Virology* 514:10. <https://doi.org/10.1186/s12985-017-0683-y>.
40. Hu Z, Zhang Y, Wang Z, Wang J, Tong Q, Wang M, Sun H, Pu J, Liu C, Liu J, Sun Y. 2019. Mouse-adapted H9N2 avian influenza virus causes systemic infection in mice. *Virology* 516:135. <https://doi.org/10.1186/s12985-019-1227-4>.
41. Peltola VT, McCullers JA. 2004. Respiratory viruses predisposing to bacterial infections: role of neuraminidase. *Pediatr Infect Dis J* 23:S87–S97. <https://doi.org/10.1097/01.inf.0000108197.81270.35>.
42. Chockalingam AK, Hickman D, Pena L, Ye J, Ferrero A, Echenique JR, Chen H, Sutton T, Perez DR. 2012. Deletions in the neuraminidase stalk region of H2N2 and H9N2 avian influenza virus subtypes do not affect postinfluenza secondary bacterial pneumonia. *J Virol* 86:3564–3573. <https://doi.org/10.1128/JVI.05809-11>.
43. McCullers JA. 2013. Do specific virus-bacteria pairings drive clinical outcomes of pneumonia? *Clin Microbiol Infect* 19:113–118. <https://doi.org/10.1111/1469-0691.12093>.
44. Peltola VT, Murti KG, McCullers JA. 2005. Influenza virus neuraminidase contributes to secondary bacterial pneumonia. *J Infect Dis* 192:249–257. <https://doi.org/10.1086/430954>.
45. Chen WH, Toapanta FR, Shirey KA, Zhang L, Giannelou A, Page C, Frieman MB, Vogel SN, Cross AS. 2012. Potential role for alternatively activated macrophages in the secondary bacterial infection during recovery from influenza. *Immunol Lett* 141:227–234. <https://doi.org/10.1016/j.imlet.2011.10.009>.
46. Didierlaurent A, Goulding J, Patel S, Snelgrove R, Low L, Bebien M, Lawrence T, van Rijt LS, Lambrecht BN, Siraad JC, Hussell T. 2008. Sustained desensitization to bacterial Toll-like receptor ligands after resolution of respiratory influenza infection. *J Exp Med* 205:323–329. <https://doi.org/10.1084/jem.20070891>.
47. van der Sluijs KF, van Elden LJ, Nijhuis M, Schuurman R, Pater JM, Florquin S, Goldman M, Jansen HM, Lutter R, van der Poll T. 2004. IL-10 is an important mediator of the enhanced susceptibility to pneumococcal pneumonia after influenza infection. *J Immunol* 172:7603–7609. <https://doi.org/10.4049/jimmunol.172.12.7603>.
48. Speshock JL, Doyon-Reale N, Rabah R, Neely MN, Roberts PC. 2007. Filamentous influenza A virus infection predisposes mice to fatal septicemia following superinfection with Streptococcus pneumoniae serotype 3. *Infect Immun* 75:3102–3111. <https://doi.org/10.1128/IAI.01943-06>.
49. Aegerter H, Kulikauskaite J, Crotta S, Patel H, Kelly G, Hessel EM, Mack M, Beinke S, Wack A. 2020. Influenza-induced monocyte-derived alveolar macrophages confer prolonged antibacterial protection. *Nat Immunol* 21:145–157. <https://doi.org/10.1038/s41590-019-0568-x>.
50. Matthias KA, Roche AM, Standish AJ, Shchepetov M, Weiser JN. 2008. Neutrophil-toxin interactions promote antigen delivery and mucosal clearance of Streptococcus pneumoniae. *J Immunol* 180:6246–6254. <https://doi.org/10.4049/jimmunol.180.9.6246>.
51. Dallaire F, Ouellet N, Bergeron Y, Turmel V, Gauthier MC, Simard M, Bergeron MG. 2001. Microbiological and inflammatory factors associated with the development of pneumococcal pneumonia. *J Infect Dis* 184:292–300. <https://doi.org/10.1086/322021>.
52. Kirby AC, Raynes JG, Kaye PM. 2005. The role played by tumor necrosis factor during localized and systemic infection with Streptococcus pneumoniae. *J Infect Dis* 191:1538–1547. <https://doi.org/10.1086/429296>.
53. Arts RJW, Moorlag S, Novakovic B, Li Y, Wang SY, Oosting M, Kumar V, Xavier RJ, Wijmenga C, Joosten LAB, Reusken C, Benn CS, Aaby P, Koopmans MP, Stunnenberg HG, van Crevel R, Netea MG. 2018. BCG vaccination protects against experimental viral infection in humans through the induction of cytokines associated with trained immunity. *Cell Host Microbe* 23:89–100.E5. <https://doi.org/10.1016/j.chom.2017.12.010>.
54. Moorlag S, Roring RJ, Joosten LAB, Netea MG. 2018. The role of the interleukin-1 family in trained immunity. *Immunol Rev* 281:28–39. <https://doi.org/10.1111/imr.12617>.
55. Mitroutis I, Ruppova K, Wang B, Chen LS, Grzybek M, Grinenko T, Eugster A, Troullinaki M, Palladini A, Kourtzelis I, Chatzigeorgiou A, Schlitzer A, Beyer M, Joosten LAB, Isermann B, Lesche M, Petzold A, Simons K, Henry I, Dahl A, Schultze JL, Wielockx B, Zamboni N, Miertschink P, Coskun U, Hajishengallis G, Netea MG, Chavakis T. 2018. Modulation of myelopoiesis progenitors is an

- integral component of trained immunity. *Cell* 172:147–161.E12. <https://doi.org/10.1016/j.cell.2017.11.034>.
56. Netea MG, Dominguez-Andres J, Barreiro LB, Chavakis T, Divangahi M, Fuchs E, Joosten LAB, van der Meer JWM, Mhlanga MM, Mulder WJM, Riksen NP, Schlitzer A, Schultze JL, Stabel Benn C, Sun JC, Xavier RJ, Latz E. 2020. Defining trained immunity and its role in health and disease. *Nat Rev Immunol* 20:375–388. <https://doi.org/10.1038/s41577-020-0285-6>.
 57. Bi J, Deng G, Dong J, Kong F, Li X, Xu Q, Zhang M, Zhao L, Qiao J. 2010. Phylogenetic and molecular characterization of H9N2 influenza isolates from chickens in Northern China from 2007–2009. *PLoS One* 5:e13063. <https://doi.org/10.1371/journal.pone.0013063>.
 58. Medina E. 2010. Murine model of pneumococcal pneumonia. *Methods Mol Biol* 602:405–410. https://doi.org/10.1007/978-1-60761-058-8_22.
 59. Tobita K, Sugiura A, Enomote C, Furuyama M. 1975. Plaque assay and primary isolation of influenza A viruses in an established line of canine kidney cells (MDCK) in the presence of trypsin. *Med Microbiol Immunol* 162:9–14. <https://doi.org/10.1007/BF02123572>.
 60. Reppe K, Radunzel P, Dietert K, Tschernig T, Wolff T, Hammerschmidt S, Gruber AD, Suttorp N, Witzernath M. 2015. Pulmonary immunostimulation with MALP-2 in influenza virus-infected mice increases survival after pneumococcal superinfection. *Infect Immun* 83:4617–4629. <https://doi.org/10.1128/IAI.00948-15>.
 61. Berger S, Goekeri C, Gupta SK, Vera J, Dietert K, Behrendt U, Lienau J, Wienhold SM, Gruber AD, Suttorp N, Witzernath M, Nouailles G. 2018. Delay in antibiotic therapy results in fatal disease outcome in murine pneumococcal pneumonia. *Crit Care* 22:287. <https://doi.org/10.1186/s13054-018-2224-5>.